Anal. Chem. **2006,** *78,* 4210−4218

Structural Analysis of Ionic Organotin(IV) Compounds Using Electrospray Tandem Mass Spectrometry

Michal Holčapek,*,† Lenka Kolářová,† Aleš Růžička,‡ Roman Jambor,‡ and Pavel Jandera†

Department of Analytical Chemistry and Department of General and Inorganic Chemistry, Faculty of Chemical Technology, University of Pardubice, nám. Čs. legií 565, 53210 Pardubice, Czech Republic

A novel electrospray ionization (ESI) mass spectrometric approach for the structure elucidation of ionic organotin(IV) compounds or complexes with weakly bonded ligands as for example monodentate carboxylates or sulfonates is proposed using both positive-ion and negative-ion ESI tandem mass spectra. The ionization mechanism of organotin(IV) compounds involves the cleavage of the most labile bond with an ionic character yielding two complementary ions, $[Cat]^+$ and $[An]^-$. Positively charged species containing tin atom, $[Cat]^+$, are analyzed in the positive-ion mode and negatively charged species without the tin atom, $[An]^-$, in the negative-ion mode. Fragmentation patterns of $[C_{24}H_{29}N_2Sn]^+$, $[C_{21}H_{22}NSn]^+$, and $[C_{17}H_{30}NSn]^+$ ions are proposed based on the detailed interpretation of MS^n spectra, which is simplified by an easy recognition of characteristic tin isotopic clusters in particular fragment ions. Proposed fragmentation mechanisms are supported by comparison with MS^n spectra of deuterium-labeled analogues. The applicability of this method is illustrated on two sets of organotin(IV) compounds, including seven [2,6-bis(dimethylaminomethyl)-phenyl]diphenyltin(IV) derivatives with small inorganic counteranions X (Br, NO_3, SCN, BF_4, SeCN, CN, PF_6), six organotin(IV) complexes containing two C,N-chelating ligands with azo dyes, and the identification of unknown hydrolysis products.

Organotin(IV) compounds exhibit interesting biological properties with important industrial and agricultural applications.[1] They are frequently used as biocides, for example, as antifouling paints on ships or wood preservatives. Other typical applications are as agricultural herbicides, fungicides, and insecticides and in industry as stabilizers for PVC or catalysts.[2−4] Their antitumor activity is also investigated in the present time.[1] The limiting factor for their further research in the medical area is a low aqueous solubility. This drawback could be improved by new organotin compounds with an ionic character, which have better solubility in water.[5] The wide range of applications and syntheses of new organotin compounds bring the need for a reliable and, if possible, fast and low-cost analytical method for their structural characterization.

Nuclear magnetic resonance (NMR) spectroscopy is an established technique for the structural analysis of organotin compounds, where the values of $\delta(^{119}Sn)$ and $^nJ(^{119}Sn,^{13}C)$ are especially important.[1] The organotin compounds containing intramolecularly coordinating Y,C,Y-chelating ligands (Y = donor-containing substituent), which represents a group of so-called hypervalent or hypercoordinated organotin(IV) compounds,[6−8] have been extensively studied to understand the properties and stereochemistry, mainly using temperature-dependent NMR spectra parameters (^1H and ^{119}Sn). The synthesis, characterization, and properties of phenyltin derivatives of 2,6-[bis(dimethylaminomethyl)phenyl]-(N,C,N-pincer) ligand[5,9,10] and some 2,6-[bis(alkyloxy)methyl]phenyl-(O,C,O) ligands[11] have been described in our recent papers with description of their mass spectra.[12]

Electrospray ionization (ESI) is one of the softest ionization techniques, which can be easily coupled to liquid-phase separation techniques, such as high-performance liquid chromatography (HPLC). The soft matter of ESI enables the molecular weight (MW) determination of many organometallic[13−15] and metal complex compounds.[16] The applications of ESI to the analysis of organotin(IV) compounds have been reported from the beginning

* Corresponding author. Phone +420-46-6037087. Fax: +420-46-6037068. E-mail: Michal.Holcapek@upce.cz; http://user.upce.cz/~holcapek/.

† Department of Analytical Chemistry.

‡ Department of General and Inorganic Chemistry.

(1) Rappoport, Z., Ed. *The chemistry of organic germanium, tin and lead compounds*; John Wiley & Sons: Ltd: New York, 2002.
(2) Pinnavaia, T. J. *Science* **1983**, *220*, 365−371.
(3) Jousseaume, B.; Laporte, C.; Rascle, M. C.; Toupance, T. *Chem. Commun.* **2003**, *12*, 1428−1429.
(4) Mascaretti, O. A.; Furlán, R. L. E. *Aldrichim. Acta* **1997**, *30*, 55−68.
(5) Růžička, A.; Dostál, L.; Jambor, R.; Buchta, V.; Brus, J.; Císařová, I.; Holčapek, M.; Holeček, J. *Appl. Organomet. Chem.* **2002**, *16*, 315−322.
(6) Smith, P. J., Ed. *Chemistry of Tin*; Blackie Academic & Professional: Glasgow, 1998.
(7) Mehring, M.; Vrasidas, I.; Horn, D.; Schürmann, M.; Jurkschat, K. *Organometallics* **2001**, *20*, 4647−4653.
(8) Beckmann, J.; Jurkschat, K.; Kaltenbrunner, U.; Rabe, S.; Schürmann, M.; Dakternieks, D.; Duthie, A.; Müller, D. *Organometallics* **2000**, *19*, 4887−4898.
(9) Růžička, A.; Jambor, R.; Brus, J.; Císařová, I.; Holeček, J. *Inorg. Chim. Acta* **2001**, *323*, 163−170.
(10) Růžička, A.; Lyčka, A.; Jambor, R.; Novák, P.; Císařová, I.; Holčapek, M.; Erben, M.; Holeček, J. *Appl. Organomet. Chem.* **2003**, *17*, 168−174.
(11) Jambor, R.; Dostál, L.; Růžička, A.; Císařová, I.; Brus, J.; Holčapek, M.; Holeček, J. *Organometallics* **2002**, *21*, 3996−4004.
(12) Kolářová, L.; Holčapek, M.; Jambor, R.; Dostál, L.; Růžička, A.; Nádvorník, M. *J. Mass Spectrom.* **2004**, *39*, 621−629.
(13) Gatlin, C. L.; Tureček, F. In *Electrospray Ionization Mass Spectrometry*; Cole, R. B., Ed.; John Wiley: New York, 1997; pp 527−570.
(14) Colton, R.; D'Agostino, A.; Traeger, J. C. *Mass Spectrom. Rev.* **1995**, *14*, 79−106.
(15) Rosenberg, E. *J. Chromatogr., A* **2003**, *1000*, 841−889.

10.1021/ac060263x CCC: $33.50
Published on Web 04/21/2006

of the electrospray era.[17] Most studies were performed on simple organotin compounds.[17−21] The potential of ESI coupling to HPLC for the sensitive quantitation of organotin pollutants[17,21,22] was investigated as well, e.g., tributyltin fragment in a sediment reference material[17] and tri- and diphenyltin and tri-, di-, and monobutyltin fragments in water.[21]

Before the advent of ESI, the conventional electron ionization (EI) was often applied in the analysis of more volatile organotin compounds. EI fragmentation patterns of simple organotin compounds with one to four aryl or alkyl substituents are described.[23−26] The typical neutral losses are alkenes, and the majority of fragment ions are even-electron ions except for the molecular radical−cation $M^{+\bullet}$ and diaryl- and dialkyltin radical ions, which is similar to the soft ionization techniques. EI mass spectra yield many fragment ions, but this advantage may also be a limiting factor of EI due to the extensive fragmentation and hence the lack of MW information. This drawback can be overcome by ESI with an ion trap analyzer, which combines the information about the MW obtained from the first-order mass spectra and additional structural information based on the MS^n analyses, as shown recently in our study of metal complexes of azo dyes.[16] The application of such an approach for studying the fragmentation behavior of more complex organotin compounds[27,28] is quite rare, and many papers oriented mainly on the synthetic aspects only claim that the structures or MWs are confirmed by ESI-MS without further reasoning. Cluster ions with more tin atoms can also be analyzed by ESI-MS,[29,30] but the isotopic patterns are very complex; therefore, the use of a high-resolution mass spectrometer, such as an ion cyclotron resonance mass spectrometer with Fourier transformation, is advantageous.[31,32]

In the present work, the ionization and fragmentation of 13 ionic organotin(IV) compounds are studied using both positive-ion and negative-ion ESI-MS and MS^n analysis using an ion trap analyzer. The goal of this study is obtaining sufficient information for the structural elucidation, which should confirm the benefits of ESI mass spectrometry for the identification of more complex organotin(IV) compounds with potential extension to other organometallic compounds.

(16) Lemr, K.; Holčapek, M.; Jandera, P.; Lyčka, A. *Rapid Commun. Mass Spectrom.* **2000**, *14*, 1881−1888.
(17) Siu, K. W. M.; Gardner, G. J.; Berman, S. S. *Anal. Chem.* **1989**, *61*, 2320−2322.
(18) Rosenberg, E.; Kmetov, V.; Grasserbauer, M. *Fresenius J. Anal. Chem.* **2000**, *366*, 400−407.
(19) Jones, T. L.; Betowski, L. D. *Rapid Commun. Mass Spectrom.* **1993**, *7*, 1003−1008.
(20) Lawson, G.; Dahm, R. H.; Ostah, N.; Woodland, E. D. *Appl. Organomet. Chem.* **1996**, *10*, 125−133.
(21) Jones-Lepp, T. L.; Varner, K. E.; McDaniel, M.; Riddick, L. *Appl. Organomet. Chem.* **1999**, *13*, 881−889.
(22) Wu, J. C.; Mester, Z.; Pawliszyn, J. *J. Anal. At, Spectrom.* **2001**, *16*, 159−165.
(23) Gielen, M.; Mayence, G. *J. Organomet. Chem.* **1968**, *12*, 363−368.
(24) Lawson, G.; Ostah, N. *Appl. Organomet. Chem.* **2000**, *14*, 383−388.
(25) Lawson, G.; Ostah, N. *Appl. Organomet. Chem.* **1993**, *7*, 183−191.
(26) Ostah, N.; Lawson, G. *Appl. Organomet. Chem.* **2000**, *14*, 874−881.
(27) Wei, J.; Miller, J. M. *J. Mass Spectrom.* **2001**, *36*, 806−815.
(28) Pellei, M.; Lobbia, G. G.; Ricciutelli, M.; Santini, C. *Polyhedron* **2003**, *22*, 499−506.
(29) Dakternieks, D.; Zhu, H.; Tiekink, E. R. T.; Colton, R. *J. Organomet. Chem.* **1994**, *476*, 33−40.
(30) Armelao, L.; Schiavon, G.; Seraglia, R.; Tondello, E.; Russo, U.; Traldi, P. *Rapid Commun. Mass Spectrom.* **2001**, *15*, 1855−1861.

EXPERIMENTAL SECTION

Organotin(IV) Compounds. All organotin(IV) compounds studied in this work (Figure 1) were synthesized in our laboratory. Their structures were confirmed by ^{1}H, ^{13}C, and ^{119}Sn NMR spectra and X-ray diffraction measurements in the solid state.[5,10,11] Prior to the mass spectrometric analysis, the organotin(IV) compounds were extracted into hexane, the solutions were evaporated to dryness, and the residue was redissolved in acetonitrile to remove nonvolatile inorganic material. Isotopically labeled standards of Cat^1 and Cat^2 (see insets in Figures 3 and 5) were synthesized to support the suggested fragmentation patterns: (a) compounds with two deuterated phenyl rings (+10 mass units), (b) compound with tetradeuterated ligand's aromatic ring and benzylic arm (+6 mass units), (c) compound with tetradeuterated ligand's aromatic ring, deuterated benzylic arm, and two deuterated phenyl rings (+16 mass units).

Instruments. ESI mass spectra were measured using an Esquire 3000 ion trap analyzer (Bruker Daltonics, Bremen, Germany). Sample solutions in acetonitrile (Merck, Darmstadt, Germany) were prepared at a concentration of ~0.1 mg/mL and analyzed by direct infusion at a flow rate of 1−3 μL/min. Mass spectra were recorded in the range from m/z 50 to 1000 (or to m/z 1500 depending on the molecular weight) in both negative-ion and positive-ion modes. The needle voltage was 4 kV in both polarity modes. The ion trap analyzer was tuned to give a maximum response for m/z 400; i.e., the tuning parameter "target mass" was set according to the expected m/z value of the analyzed ion. The ion source temperature was 300 °C; the flow rate and the pressure of nitrogen were 4 L/min and 10 psi, respectively. The isolation width for MS^n experiments was $\Delta m/z = 8$, and the collision amplitude (CA) was selected depending on the stability of the particular fragment ion in the range 0.6−1 V. The negative-ion ESI mass spectra of small inorganic anions with m/z lower than m/z 100 were measured on a Platform quadrupole analyzer (Micromass) with the following settings: mass range m/z 35−600, ion source temperature 100 °C, cone voltage 30 V, and flow rate 10 μL/min.

Positive-Ion Electrospray Ionization Mass Spectra. (1) [2,6-Bis(dimethylaminomethyl)phenyl]diphenyltin(IV) (Cat^1, Figure 3A). The experimental and theoretical isotopic abundances for the cationic part of the molecule $[C_{24}H_{29}N_2Sn]^+$ in the positive-ion ESI mode were compared in Figure 2. No other ions were observed in the first-order ESI mass spectra. The interpretation of MS^n spectra was summarized in Table 1.

Deuterium-Labeled D_{10}-Cat^1 (Figure 3B). Positive-ion MS^2 of 475 (CA 1.0): m/z 430, $[Cat - CH_3NHCH_3]^+$, 9%; m/z 392, $[Cat - C_6HD_5]^+$, 15%; m/z 349, $[Cat - C_6HD_5 - CH_3NCH_2]^+$, 100%; m/z 303, $[Cat - C_6HD_5 - CH_3NDCH_3 - CH_3NCH_2]^+$, 44%; m/z 272, $[Cat - C_6HD_5 - Sn]^+$, 17%; m/z 229, $[Cat - C_6HD_5 - Sn - CH_3NCH_2]^+$, 34%; m/z 186, $[Cat - C_6HD_5 - Sn - 2*CH_3NCH_2]^+$, 8%; m/z 170, $[Cat - C_6HD_5 - Sn - CH_3NCH_2 - (CH_3)_2NCHD]^+$, 3%.

(2) [(2-Dimethylaminomethyl)phenyl]diphenyltin(IV) (Cat^2, Figure 5A). Positive-ion ESI-MS (theoretical relative abundances in parentheses): m/z 404, 45% (41%); m/z 405, 31% (32%); m/z 406, 79% (75%); m/z 407, 41% (41%); m/z 408, 100% (100%); m/z 409, 23% (23%); m/z 410, 17% (16%); m/z 411, 5% (3%); m/z 412, 15% (17%) and m/z 413, 4% (4%). The interpretation of MS^n spectra was summarized in Table 2.

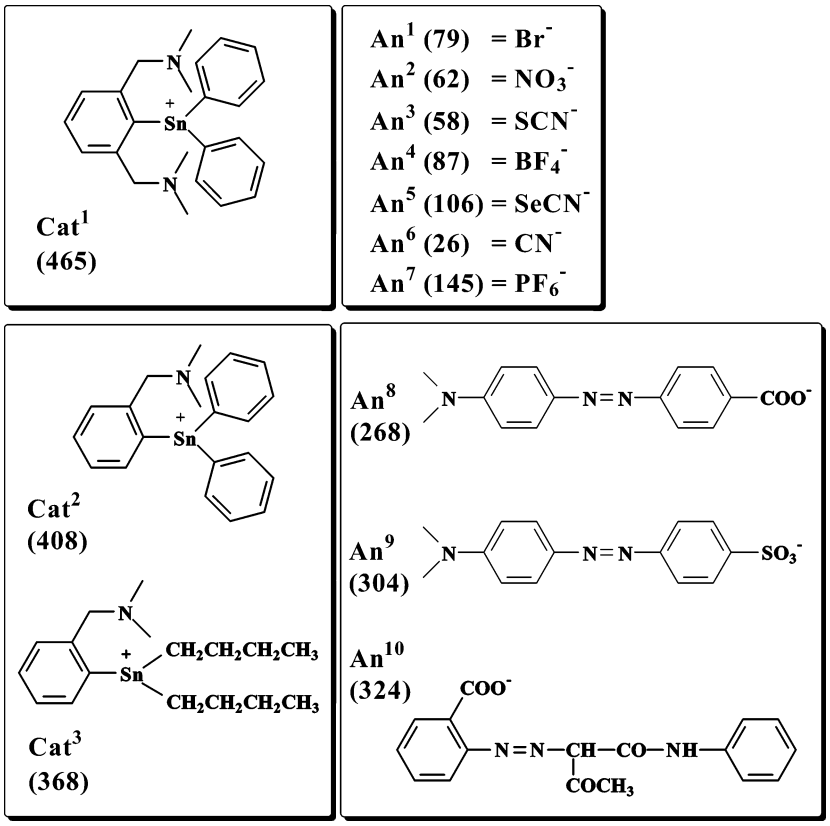

Figure 1. Structures of cationic and anionic parts of organotin(IV) compounds with their *m*/*z* values in parentheses.

Table 1. Relative Abundances of Fragment Ions (in %) Measured in MS^n Experiments of the Cationic Part Cat^1 [$C_{24}H_{29}N_2Sn$]$^+$ and of Other Precursor Ions (PI)[a]

m/*z*	ion structure	MS^2 of 465	MS^3 of 465−420	MS^3 of 465−387	MS^3 of 465−344	MS^4 of 465−344−299	MS^4 of 465−344−224	MS^4 of 465−344−181
420	[Cat−CH_3NHCH_3]$^+$	11	PI					
387	[Cat−C_6H_6]$^+$	20		PI				
375	[Cat−2*CH_3NHCH_3]$^+$		18					
360	[Cat−C_6H_6−HCN]$^+$			13				
344	[Cat−C_6H_6−$CH_3N{=}CH_2$]$^+$	100		100	PI			
301	[Cat−2*$CH_3N{=}CH_2$−C_6H_6]$^+$		99					
299	[Cat−C_6H_6−CH_3NHCH_3−$CH_3N{=}CH_2$]$^+$	38		50	37	PI		
267	[Cat−C_6H_6−Sn]$^+$	8		10				
257	[Cat−CH_3NHCH_3−$CH_3N{=}CH_2$−Sn]$^+$		100					
242	[Cat−CH_3NHCH_3−$(CH_3)_2NCH_2$−Sn]$^+$·		8					
224	[Cat−C_6H_6−Sn−$CH_3N{=}CH_2$]$^+$	12		4	100		PI	
179	[Cat−C_6H_6−Sn−CH_3NHCH_3−$CH_3N{=}CH_2$]$^+$	−	24			100		
181	[Cat−C_6H_6−Sn−2*$CH_3N{=}CH_2$]$^+$	9			71	20	100	PI
166	[Cat−C_6H_6−Sn−$CH_3N{=}CH_2$−$(CH_3)_2NCH_2$]$^+$·	3			15	16	3	100

[a] Collision amplitude is 0.8 V, except for *m*/*z* 387 (0.65 V) and 344 (1.0 V).

Deuterium-Labeled D_6-Cat^2 (Figure 5B). Positive-ion ESI-MS (theoretical relative abundances in parentheses): *m*/*z* 410, 36% (41%); *m*/*z* 411, 39% (32%); *m*/*z* 412, 77% (75%); *m*/*z* 413, 47% (41%); *m*/*z* 414, 100% (100%); *m*/*z* 415, 22% (23%); *m*/*z* 416, 24% (16%); *m*/*z* 417, 4% (3%); *m*/*z* 418, 14% (17%), and *m*/*z* 419, 4% (4%). Positive-ion MS^2 of 414 (CA 1.0): *m*/*z* 369, [Cat − CH_3NHCH_3]$^+$, 100%; *m*/*z* 336, [Cat − C_6H_6]$^+$, 27%; *m*/*z* 290, [Cat − C_6H_5D − CH_3NHCH_3]$^+$, 72%; *m*/*z* 249, [Cat − CH_3NHCH_3 − Sn]$^+$, 16%; *m*/*z* 238, [Cat − C_6H_6 − $C_7H_2D_6$]$^+$, 14%; *m*/*z* 216, [Cat − C_6H_6 − Sn]$^+$, 25%; *m*/*z* 197, [C_6H_5Sn]$^+$, 24%; *m*/*z* 173, [Cat − C_6H_6 − Sn − CH_3NCH_2]$^+$, 10%; *m*/*z* 170, [Cat − CH_3NHCH_3 − C_6H_5D-Sn]$^+$, 11%.

Deuterium-Labeled D_{10}-Cat^2 (Figure 5C). Positive-ion ESI-MS (theoretical relative abundances in parentheses): *m*/*z* 414, 39% (41%); *m*/*z* 415, 29% (32%); *m*/*z* 416, 72% (75%); *m*/*z* 417, 44% (41%); *m*/*z* 418, 100% (100%); *m*/*z* 419, 25% (23%); *m*/*z* 420, 17% (16%); *m*/*z* 421, 5% (3%); *m*/*z* 422, 19% (17%) and *m*/*z* 423, 5% (4%). Positive-ion MS^2 of 418 (CA 1.0): *m*/*z* 372, [Cat − CH_3NDCH_3]$^+$, 100%; *m*/*z* 335, [Cat − C_6HD_5]$^+$, 43%; *m*/*z* 289, [Cat − CH_3NDCH_3 − C_6HD_5]$^+$, 96%; *m*/*z* 252, [Cat − CH_3NDCH_3 − Sn]$^+$, 32%; *m*/*z* 241, [Cat − C_6HD_5 − $C_7H_6D_2$]$^+$, 14%; *m*/*z* 215, [Cat − C_6HD_5 − Sn]$^+$, 56%; *m*/*z* 202, [C_6D_5Sn]$^+$, 19%; *m*/*z* 172, [Cat − C_6HD_5 − Sn − CH_3NCH_2]$^+$, 41%; *m*/*z* 169, [Cat − CH_3NDCH_3 − C_6HD_5 − Sn]$^+$, 16%.

Table 2. Relative Abundances of Fragment Ions (in %) Measured in MS^n Experiments of the Cationic Part Cat² $[C_{21}H_{22}NSn]^+$ (*m/z* 408) and of Other Precursor Ions (PI)[a]

m/z	ion structure	MS^2 of 408	MS^3 of 408−363	MS^3 of 408−285	MS^3 of 408−243
363	$[Cat-CH_3NHCH_3]^+$	100	PI		
330	$[Cat-C_6H_6]^+$	20			
285	$[Cat-C_6H_6-CH_3NHCH_3]^+$	67	12	PI	–
243	$[Cat-CH_3NHCH_3-Sn]^+$	31	100		PI
238	$[Cat-C_6H_6-C_6H_5CH_3]^+$	10			
228	$[Cat-CH_3NHCH_3-Sn-CH_3]^{+\bullet}$				14
210	$[Cat-C_6H_6-Sn]^+$	28			
197	$[C_6H_5Sn]^+$	13	9		
165	$[Cat-C_6H_6-Sn-CH_3NHCH_3]^+$	20	11	100	100
120	$[Sn]^{+\bullet}$			2	

[a] Collision amplitude is 1.0 V for *m/z* 408 and 0.9 V for *m/z* 363, 285, and 243.

Table 3. Relative Abundances of Fragment Ions (in %) Measured in MS^n Experiments of the Cationic Part Cat³ $[C_{17}H_{30}NSn]^+$ (*m/z* 368) and of Other Precursor Ions (PI)[a]

m/z	ion structure	MS^2 of 368	MS^3 of 368−312	MS^3 of 368−254
312	$[Cat-butene]^+$	20	PI	
254	$[Cat-butene-butane]^+$	100	43	PI
233	$[CH_3(CH_2)_3(CH_3(CH_2)_2CH)Sn]^+$	3		
211	$[Cat-butene-butane-CH_3NCH_2]^+$	3		
209	$[Cat-butene-butane-CH_3NHCH_3]^+$			3
177	$[CH_3(CH_2)_3Sn]^+$	10		
134	$[Cat-butene-butane-Sn]^+$	73	100	100
91	$[Cat-butene-butane-Sn-CH_3NCH_2]^+$			15

[a] Collision amplitude is 1.0 V, except for *m/z* 254 (0.8 V).

Deuterium-Labeled D_{16}-Cat² (Figure 5D). Positive-ion ESI-MS (theoretical relative abundances in parentheses): *m/z* 420, 44% (41%); *m/z* 421, 34% (32%); *m/z* 422, 74% (75%); *m/z* 423, 49% (41%); *m/z* 424, 100% (100%); *m/z* 425, 23% (23%); *m/z* 426, 13% (16%); *m/z* 427, 4% (3%); *m/z* 428, 16% (17%) and *m/z* 429, 3% (4%). Positive-ion MS^2 of 424 (CA 1.0): *m/z* 378, $[Cat - CH_3NDCH_3]^+$, 100%; *m/z* 341, $[Cat - C_6HD_5]^+$, 38%; *m/z* 294, $[Cat - C_6D_6 - CH_3NDCH_3]^+$, 92%; *m/z* 258, $[Cat - CH_3NDCH_3 - Sn]^+$, 29%; *m/z* 242, $[Cat - C_6HD_5 - C_7HD_7]^+$, 36%; *m/z* 221, $[Cat - C_6HD_5 - Sn]^+$, 45%; *m/z* 202, $[C_6D_5Sn]^+$, 42%; *m/z* 178, $[Cat - C_6HD_5 - Sn - CH_3NCH_2]^+$, 20%; *m/z* 174, $[Cat - CH_3NDCH_3 - C_6D_6 - Sn]^+$, 30%.

Hydrolysis Products of Cat²Cl (Figure 7A−C). Positive-ion MS: *m/z* 1284, $[(CatO)_3C]^+$, 100%; *m/z* 833, $[CatOCat + H]^+$, 4%; *m/z* 408, $[Cat]^+$, 2%. Positive-ion MS^2 of 1284 (CA 1.0): *m/z* 408, $[Cat]^+$, 100%; *m/z* 363, $[Cat - CH_3NHCH_3]^+$, 5%. Positive-ion MS^3 of 1284−408 (CA 1.0−0.9): *m/z* 363, $[Cat - CH_3NHCH_3]^+$, 100%; *m/z* 330, $[Cat - C_6H_6]^+$, 29%; *m/z* 285, $[Cat - C_6H_6 - CH_3NHCH_3]^+$, 70%; *m/z* 243, $[Cat - CH_3NHCH_3 - Sn]^+$, 26%; *m/z* 238, $[Cat - C_6H_6 - C_6H_5CH_3]^+$, 13%; *m/z* 210, $[Cat - C_6H_6 - Sn]^+$, 27%; *m/z* 197, $[C_6H_5Sn]^+$, 12%; *m/z* 165, $[Cat - C_6H_6 - Sn - CH_3NHCH_3]^+$, 14%.

Hydrolysis Products of D_{16}-Cat²Cl (Figure 7D). Positive-ion MS: *m/z* 1332, $[(CatO)_3C]^+$, 100%; *m/z* 865, $[CatOCat + H]^+$, 39%; *m/z* 424, $[Cat]^+$, 4%. Positive-ion MS^2 of 1332 (CA 1.0): *m/z* 424, $[Cat]^+$, 100%; *m/z* 378, $[Cat - CH_3NDCH_3]^+$, 3%. Positive-ion MS^3 of 1332−424 (CA 1.0−0.9): *m/z* 378, $[Cat - CH_3NDCH_3]^+$, 100%; *m/z* 341, $[Cat - C_6HD_5]^+$, 26%; *m/z* 294, $[Cat - C_6D_6 - CH_3NDCH_3]^+$, 42%; *m/z* 258, $[Cat - CH_3NDCH_3 - Sn]^+$, 18%; *m/z* 242, $[Cat - C_6HD_5 - C_7HD_7]^+$, 19%; *m/z* 221, $[Cat - C_6HD_5 - Sn]^+$,25%; *m/z* 202, $[C_6D_5Sn]^+$, 25%; *m/z* 178, $[Cat - C_6HD_5 - Sn - CH_3NCH_2]^+$, 23%; *m/z* 174, $[Cat - CH_3NDCH_3 - C_6D_6 - Sn]^+$, 22%.

(3) [(2-Dimethylaminomethyl)phenyl]dibutyltin(IV) (Cat³). Positive-ion ESI-MS (theoretical relative abundances in parentheses): *m/z* 364, 44% (42%); *m/z* 365, 30% (30%); *m/z* 366, 70% (75%); *m/z* 367, 39% (39%); *m/z* 368, 100% (100%); *m/z* 369, 20% (19%); *m/z* 370, 11% (15%); *m/z* 371, 3% (3%); *m/z* 372, 15% (17%) and *m/z* 373, 3% (3%). The interpretation of MS^n spectra was summarized in Table 3.

Negative-Ion Electrospray Ionization Mass Spectra. (1) Small Inorganic Anions. Only first-order negative-ion ESI mass spectra were measured for small inorganic anions: Br, *m/z* 79 and 81, experimental relative abundances 99:100% (theoretically 100:97%); NO_3, *m/z* 62, 100% (100%); SCN, *m/z* 58:59:60, 100:2:4% (100:2:4%); BF_4, *m/z* 86:87, 26:100% (25:100%); SeCN, *m/z* 102: 103:104:106, 12:9:35:100:20% (18:15:48:100:18%); CN, *m/z* 26, 100% (100%); PF_6, *m/z* 145, 100% (100%).

(2) Azo Dye Anions. 4-{[4′-(Dimethylamino)phenyl]azo}benzoate (An,[8] Figure S-6). Negative-ion ESI-MS: *m/z* 268, $[An]^-$, 100%; *m/z* 555. Negative-ion MS^2 of 268 (CA 0.7): *m/z* 224, $[An - CO_2]^-$, 100%; *m/z* 193, $[An - CO_2 - CH_3NH_2]^-$, 3%; *m/z* 182, $[An - CO_2 - CH_2NCH_2]^{-\bullet}$, 88%; *m/z* 92, $[C_6H_5NH]^-$, 5%.

4-{[4′-(Dimethylamino)phenyl]azo}benzenesulfonate (An,[9] Figure S-7). Negative-ion ESI-MS: *m/z* 304, $[An]^-$, 100%; *m/z* 631. Negative-ion MS^2 of 304 (CA 0.8): *m/z* 289, $[An - CH_3]^{-\bullet}$, 38%; *m/z* 260, $[An - CH_3NCH_3]^{-\bullet}$, 3%; *m/z* 240, $[An - SO_2]^-$, 38%; *m/z* 225, $[An - SO_2 - CH_3]^{-\bullet}$, 14%; *m/z* 156, $[C_6H_4SO_3]^{-\bullet}$, 100%. Negative-ion MS^3 of 304−289 (CA 0.8−0.8): *m/z* 260, $[An - CH_3NCH_3]^{-\bullet}$, 100%; *m/z* 246, $[An - CH_3NCH_3 - N]^-$, 7%; *m/z*

224, [An − HSO_2 − CH_3]$^-$, 76%; *m/z* 156, [$C_6H_4SO_3$]$^{-\bullet}$, 82%. Negative-ion MS^3 of 304−240 (CA 0.8−0.7): *m/z* 225, [An − SO_2 − CH_3]$^{-\bullet}$, 100%. Negative-ion MS^3 of 304−156 (CA 0.8−0.6): *m/z* 95, [CH_3SO_3]$^-$, 94%; *m/z* 80, [SO_3]$^{-\bullet}$, 100%; *m/z* 64, [SO_2]$^{-\bullet}$, 12%. Negative-ion MS^4 of 304−289−260 (CA 0.8−0.8−0.7): *m/z* 246, [An − CH_3NCH_3 − N]$^-$, 98%; *m/z* 196, [An − SO_2 − CH_3NCH_3]$^{-\bullet}$, 100%; *m/z* 166, [An − CH_3NCH_3 − SO_3 − N]$^-$, 34%; *m/z* 156, [$C_6H_4SO_3$]$^{-\bullet}$, 29%.

2-{[*N*′-(2-Oxo-1-phenylcarbamoylpropyliden)hydrazo]}-benzoate (An^{10}, Figure S-8). Negative-ion ESI-MS: *m/z* 324, [An]$^-$, 100%; *m/z* 671. Negative-ion MS^2 of 324 (CA 0.9): *m/z* 280, [An − CO_2]$^-$, 100%; *m/z* 205, [An − CO_2 − C_6H_3]$^{-\bullet}$, 59%; *m/z* 176, [$C_6H_5NHCOCH(COCH_3)$]$^-$, 19%; *m/z* 161, [C_6H_5-$NHCOCHCO$]$^{-\bullet}$, 6%; *m/z* 134, [$C_6H_5NHCOCH_2$]$^-$, 3%; *m/z* 92, [C_6H_5NH]$^-$, 3%.

RESULTS AND DISCUSSION

Analytical Methodology. Figure 1 shows the cationic ("Cat") and anionic ("An") parts of ionic organotin(IV) compounds synthesized and analyzed in this work: Cat^1 with An^1−An^7, Cat^2 with An^8−An^{10}, and Cat^3 with An^8−An^{10}. Mass spectra for the cationic part (i.e., Cat^1, Cat^2, and Cat^3) in the positive-ion mode are independent of the type of anionic part. Similarly, each anionic part yields the same results in the negative-ion mode regardless of the type of cationic counterion, which allows a separate discussion of results for both polarity modes. All organotin(IV) compounds studied were first extracted into hexane as a nonpolar solvent to avoid possible interferences from inorganic ions potentially present in synthesized samples.

Unlike most organic and bioorganic compounds, the organotin-(IV) compounds studied usually do not provide (de)protonated molecules or molecular adducts in the first-order mass spectra; hence, the information on MWs cannot be obtained directly from the spectra. This significant drawback can be overcome by measuring both positive-ion and negative-ion mass spectra, which yields complementary information about the cationic and anionic parts of the molecules. The sum of masses of two parts corresponds to the MW. In subsequent MS^n analyses, many characteristic fragment ions can be found and correlated with the structures. The characteristic isotopic distribution of the tin atom allows clear proof of the presence or absence of tin in particular fragment ions. The first-order mass spectra yield only [Cat]$^+$ in the positive-ion mode and [An]$^-$ in the negative-ion mode mostly without any fragment ions; therefore, no first-order spectra are presented here and observed ions are listed in Experimental Section. Only a few additional ions are observed in the first-order mass spectra as discussed in the following section.

Positive-Ion ESI-MS. Positive-ion first-order and MS^n spectra are identical for all studied compounds Cat^{1}An^1−Cat^{1}An^7 with the same cationic part of molecules (Table 1). Only the [$C_{24}H_{29}N_2$-Sn]$^+$ ion (cationic part, "Cat^1") is observed in the positive-ion mode; fragment ions are missing. Figure 2 illustrates a good correlation between the theoretically calculated and experimentally measured isotopical abundances of [$C_{24}H_{29}N_2Sn$]$^+$ ion. This correlation is used as Supporting Information for the suggestion of composition of individual ions, which is useful mainly for unknown ions containing more tin atoms, such as hydrolysis products.

MS^2 of the precursor ion at *m/z* 465 yields a fragment-rich product mass spectrum (Figure 3A), which can be correlated with

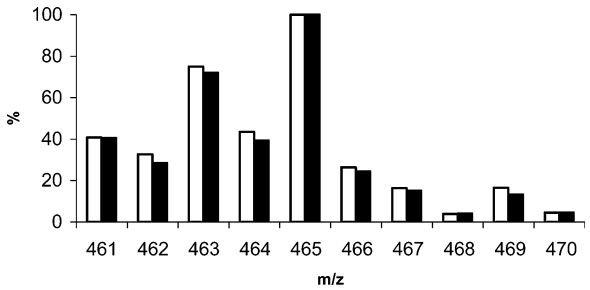

Figure 2. Comparison of theoretical (left white bars) and experimental (right black bars) isotopic abundances of the cationic part [$C_{24}H_{29}N_2Sn$]$^+$ measured with positive-ion ESI-MS.

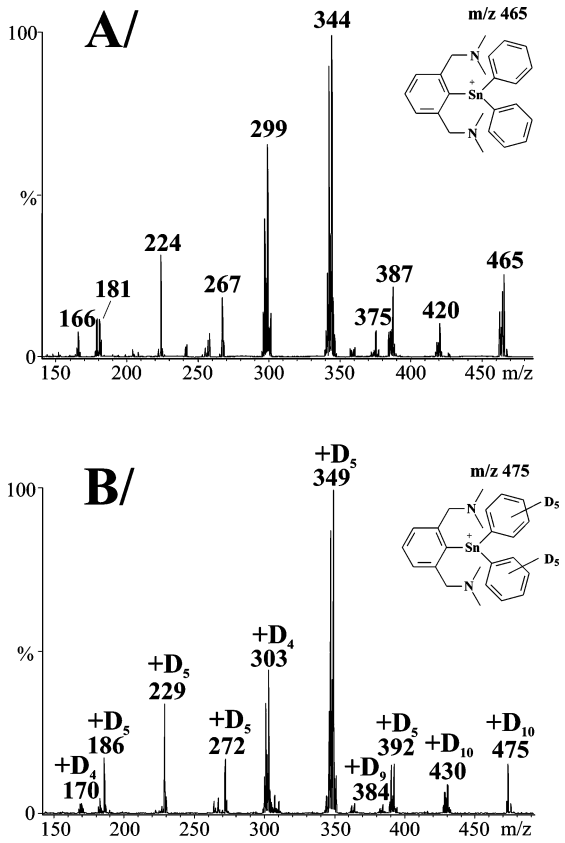

Figure 3. Positive-ion ESI-MS/MS spectra of (A) precursor ion [$C_{24}H_{29}N_2Sn$]$^+$ at *m/z* 465 (Cat^1) and (B) its D_{10}-labeled analogue deuterated on two phenyl rings (D_{10}-Cat^1).

the structure, because the fragmentation behavior is well predictable. All tin-containing fragment ions show a characteristic isotopic pattern, i.e., the ions at *m/z* 465, 420, 387, 344, and 299, while the fragment ions without tin can be easily recognized as well, i.e., *m/z* 267, 224, 181, and 166. The complete fragmentation pattern of the [$C_{24}H_{29}N_2Sn$]$^+$ ion is proposed on the basis of detailed interpretation of MS^n spectra (Figure 4). All fragmentation steps are confirmed by MS/MS measurements of particular fragment ions (see Table 1). Characteristic neutral losses are attributed to CH_3NHCH_3 (Δ*m/z* 45), $CH_3N{=}CH_2$ (Δ*m/z* 43), C_6H_6 (Δ*m/z* 78), and Sn (Δ*m/z* 120). To confirm structures of fragment ions, deuterated standards in well-defined positions have been synthesized to give a better insight into the fragmentation mechanism, as shown on the example of labeled analogue of Cat^1 with 10 deuterium atoms on two phenyl rings (Figure 3B). The comparison of Figure 3A and B shows the number of deuterium atoms in

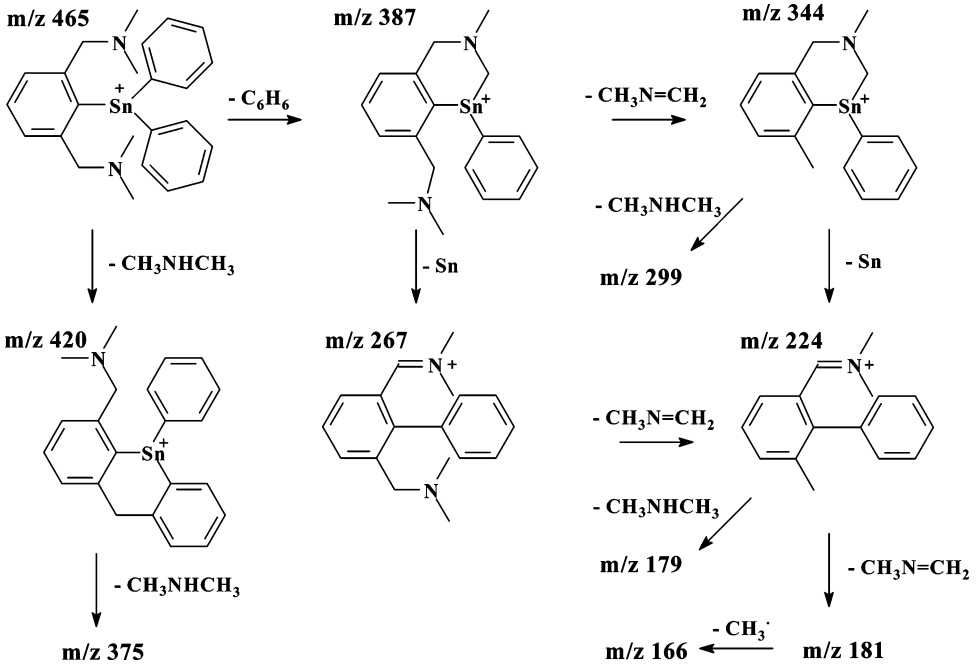

Figure 4. Fragmentation mechanism of the cationic part $[C_{24}H_{29}N_2Sn]^+$ (Cat^1) based on the interpretation of ESI-MS^n spectra.

individual fragment ions, which supports the suggested fragmentation pattern (Figure 4). All observed ions are even-electron ions except for *m/z* 166.

Similar fragmentation patterns are proposed for Cat^2 (Figures S-1−S-4 in Supporting Information) and Cat^3 (Figure S-5). Unlike Cat^1, the protonated molecules and the molecular adducts with sodium and potassium ions are observed with low relative abundances in addition to the $[Cat]^+$ ions. The relative abundances of $[M + Na]^+$ and $[M + K]^+$ ions are influenced by the salt content in samples and solvents used for mass spectrometric analyses. The typical neutral loss for butyl-substituted tin(IV) compounds (e.g., Cat^3) is butene followed by the loss of butane from the second butyl group. Similarly to the spectra of Cat^1, the majority of ions are even-electron ions except for some odd-electron ions with low relative abundance in the case of Cat^2, i.e., *m/z* 228 and 120. The detailed interpretation and relative abundances of fragment ions in MS^n spectra for Cat^2 and Cat^3 are listed in Tables 2 and 3. The results for Cat^2 are supported by MS^n measurements of deuterium-labeled standards, as shown in the examples of compounds with deuterated benzyl group D_6-Cat^2 (Figure 5B), deuterated both phenyl rings D_{10}-Cat^2 (Figure 5C), and deuterated all benzyl and phenyl groups D_{16}-Cat^2 (Figure 5D). The mass shifts in particular tandem mass spectra confirm proposed fragmentation mechanisms, but in some cases, the main peaks are accompanied by less abundant peaks with a different number of deuterium atoms. For example, the neutral loss of CH_3NHCH_3 comes from the rearrangement of one hydrogen/deuterium atom from a phenyl ring (compare transitions *m/z* 414−369 in Figure 5B, *m/z* 418−372 in Figure 5C, and *m/z* 424−378 in Figure 5D); the benzene loss corresponds to the phenyl plus one hydrogen from the dimethylamino group, because the neutral loss $\Delta m/z$ 78 is observed in Figure 5A (*m/z* 408−330 and 363−285) and 5B (*m/z* 414−336) and $\Delta m/z$ 83 in Figure 5C (*m/z* 418−335 and 372−289) and D (*m/z* 424−341), etc. The fragmentation mechanism for Cat^2 (Figure S-1) and its labeled analogues with D_6 (Figure S-2), D_{10} (Figure S-3), and D_{16} (Figure S-4) are shown in Supporting Information.

Negative-Ion ESI-MS. (1) Small Inorganic Anions. Mass spectra of small inorganic ions are trivial (see Experimental Section), but they provide valuable structure confirmation on anionic parts of studied organotin compounds, which cannot be obtained from NMR spectra. ESI mass spectra can also be used for monitoring the conversion of bromide derivative to the target anion by comparing the sum of all intensities for target anion (e.g., *m/z* 102, 103, 104, 106, and 108 for SeCN) with the initial bromide (i.e., *m/z* 79 and 81). A quadrupole analyzer is preferred for ions with masses lower than *m/z* 100, because the isotopic ratios of low-mass anions measured using an ion trap are inaccurate and the sensitivity is significantly decreased in the low-mass region. For masses lower than *m/z* 60, the quadrupole analyzer is the only choice, because no signal is obtained with an ion trap. The experimental isotopic patterns are always compared with the theoretical calculation to confirm the identification of inorganic anions containing atoms with more abundant natural isotopes, for example bromine, boron, and selenium atoms.

(2) Azo Dye Anions. The negative-ion ESI mass spectra of azo dyes sulfonate and benzoate complexes with organotin(IV) compounds are identical to the mass spectra of azo dyes alone. In addition to negatively charged ions corresponding to the ionic parts $[An]^-$, dimeric ions $[2*An + Na]^-$ are also formed in a gas phase with the relative abundances in the range of 1−6%. The observed ions for anionic parts An,[8] An[9], and An[10] are listed in Experimental Section. The complete fragmentation patterns for An[8] (Figure S-6), An[9] (Figure S-7), and An[10] (Figure S-8) are shown in Supporting Information. The typical neutral losses are CH_2=

(31) Jackson, P.; Fisher, K. J.; Dance, I. G.; Gadd, G. E.; Willett, G. D. *J. Cluster Sci.* **2002**, *13*, 165−166.
(32) Jackson, P.; Dance, I. G.; Fisher, K. J.; Willett, G. D.; Gadd, G. E. *Int. J. Mass Spectrom. Ion Processes* **1996**, *158*, 329−337.

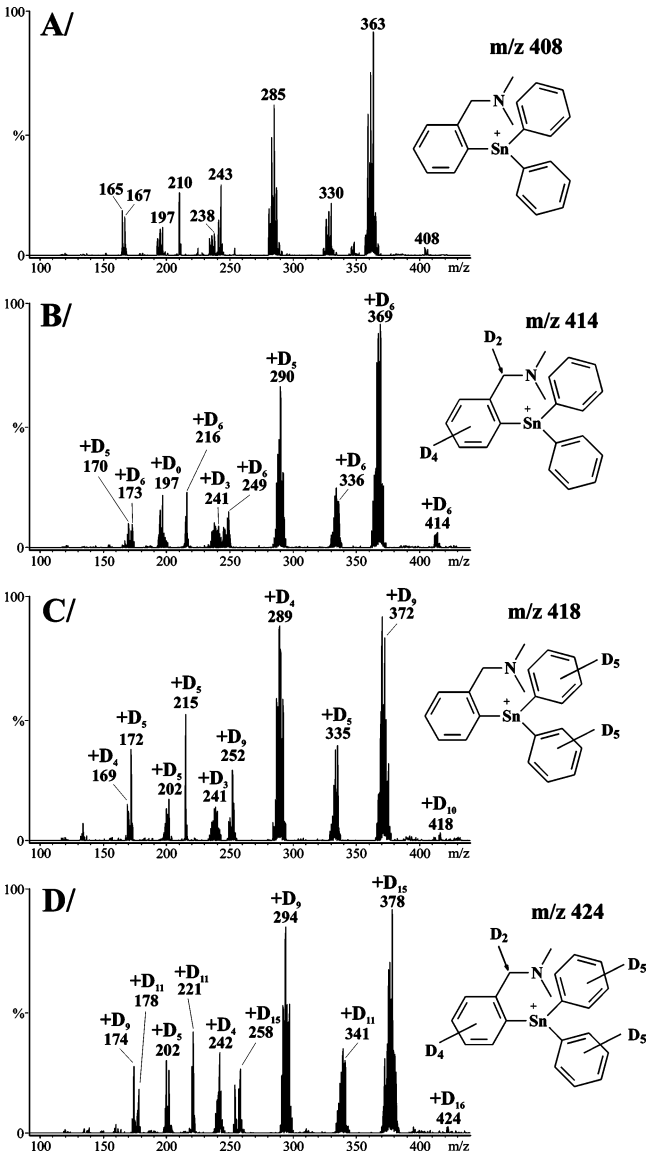

Figure 5. Positive-ion ESI-MS/MS spectra of (A) precursor ion $[C_{21}H_{22}NSn]^+$ at *m*/*z* 408 (Cat^2) amd (B) its D_6-Cat^2-, (C) D_{10}-Cat^2-, and (D) D_{16}-Cat^2-labeled analogues.

NH ($\Delta m/z$ 29) and methyl radical, which yields abundant odd-electron ions in the ESI mass spectra contradicting the even-electron rule.[32] This phenomenon is already known from our previous studies of the fragmentation behavior of azo dyes.[33−35] The typical neutral loss for carboxylic acids is CO_2 ($\Delta m/z$ 44).

Identification of Hydrolysis Products. The applications of organotin(IV) compounds in biological and catalytic processes are almost exclusively linked together with the use of tri- and diorganotin halides and products of their hydrolysis, but the structures of such hydrolytic products are usually polymeric or unknown.[4,6] In our experiments, the hydrolysis of triorganotin chloride bearing the C,N-chelating ligand has been studied due to its known monomerization ability[37] to simplify the products. Nonlabeled and three isotopically labeled compounds (D_6, D_{10}, D_{16}) of general formula Cat^2Cl (Figure 5) have been treated with aqueous NaOH. The measurements of ESI-MS^n, multinuclear NMR, X-ray diffraction, infrared spectroscopy, and cryoscopy in benzene confirm the presence of three main products (Figure 6) depending on conditions: the presence of air, the concentration of NaOH, the concentration of sample, the type of solvent, and temperature.[38]

In all ESI-MS spectra, species I and II (Figure 6) are observed immediately after mixing the reaction mixture under argon atmosphere. After exposing crystals (exclusively the species II) or an equilibrium of I and II in the solution to air, the relative concentration of species I decreases and new species III is formed in a few hours. Triorganotin carbonate(III) is observed in the mass spectra as an adduct with another Cat^2 as species IV (Figures 6 and 7).

The base peak of the first-order spectrum of hydrolysis products of Cat^2Cl (Figure 7A) is the peak of species IV at *m*/*z* 1280 for the centroid peak, which is shifted by four mass units from the monoisotopic peak at *m*/*z* 1284. The peaks of other ions (Cat, II and *m*/*z* 465) have low relative abundances (below 5%). In MS/MS spectra of *m*/*z* 1284 (Figure 7B), the base peak corresponds to $[Cat]^+$ at *m*/*z* 408. Tandem mass spectra of ion at *m*/*z* 465 (Figure 7C) confirm that this ion differs from Cat^1 (compare MS/MS spectra of *m*/*z* 465 in Figures 7C and 3A), and the only logical explanation is the structure shown in Figure 7C formed by the migration of C−N chelating ligand between two species. Figure 7D depicts the spectrum of hydrolysis product of D_{16} labeled Cat^2Cl yielding D_{48} shifted species IV. The extensive series of multistage tandem mass spectrometric experiments (not shown) confirm that proposed structures and hydrolysis reaction mechanism are correct. In all cases, the observed isotopic patterns for ions containing one, two, or three tin atoms fit well with theoretically calculated values. In addition to deuterium-labeled compounds, the hydrolysis reactions have also been performed with the structural analogues of Cat^2Cl, where phenyl groups are replaced by methyl, *n*-butyl, or *tert*-butyl substituents. The same hydrolysis products are obtained in all cases except for the *tert*-butyl analogue, where the main observed products are species I and II. The results obtained for all studied substituents (phenyl, methyl, *n*-butyl, *tert*-butyl) are listed in Table 4 together with *m*/*z* values of observed ions and their relative abundances in percent. The hydrolysis reaction products are the same for phenyl, methyl, and *n*-butyl substitution, but it differs for a *tert*-butyl substituent probably for steric reasons. These results demonstrate that this approach is suitable for structural studies of complex hydrolysis products of organotin compounds in mixtures even without a chromatographic separation or other purification step.

CONCLUSIONS

Complementary information from positive-ion and negative-ion ESI mass spectra is valuable for the structural analysis of organotin(IV) compounds and potentially for other organometallic compounds that do not give molecular ions in the first-order mass spectra. Positive-ion ESI mass spectra provide information about the cationic parts of the molecules, while the negative-ion ESI

(33) Karni, A.; Mandelbaum, A. *Org. Mass Spectrom.* **1980**, *15*, 53−64.
(34) Holčapek, M.; Jandera, P.; Přikryl, J. *Dyes Pigm.* **1999**, *43*, 127−137.
(35) Holčapek, M.; Jandera, P.; Zderadička, P. *J. Chromatogr., A* **2001**, *926*, 175−186.
(36) Ansorgová, D.; Holčapek, M.; Jandera, P. *J. Sep. Sci.* **2003**, *26*, 1017−1027.
(37) Bareš, J.; Novák, P.; Jambor, R.; Nádvorník, M.; Lébl, T.; Císařová, I.; Růžička, A.; Holeček, J. *Organometallics* **2004**, *23*, 2967−2971.
(38) Padělková, Z. Diploma Thesis, University of Pardubice, Faculty of Chemical Technology, Czech Republic, 2004.

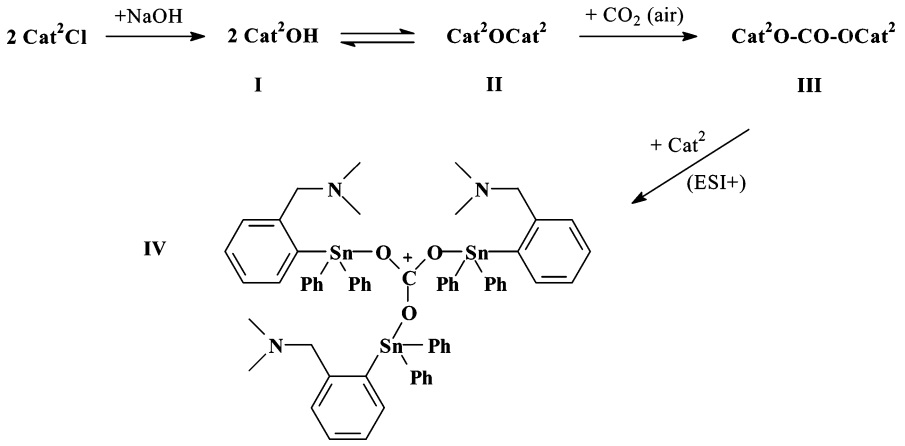

Figure 6. Proposed mechanism of hydrolysis reaction of Cat^2Cl and the structure of final hydrolysis product III and species IV observed in ESI mass spectra.

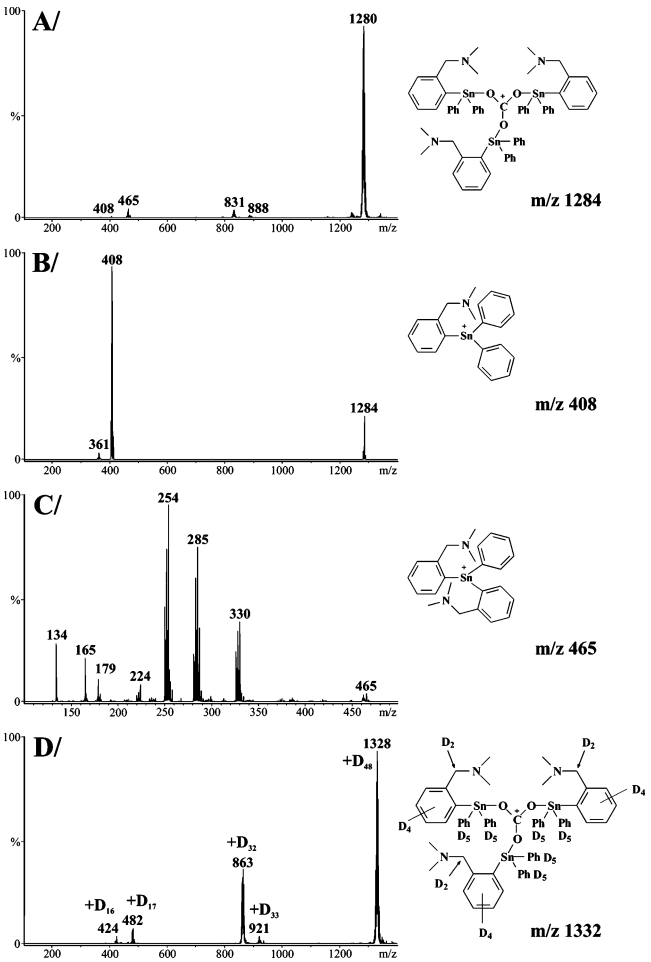

Figure 7. Positive-ion ESI mass spectra of hydrolysis product of Cat^2Cl: (A) first-order spectrum, (B) MS/MS spectrum of *m*/*z* 1284, (C) MS/MS spectrum of *m*/*z* 465, and (D) first-order spectrum of labeled D_{48} analogue.

Table 4. Relative Abundances of Ions (in %) Observed in Positive-Ion First-Order Mass Spectra of Hydrolysis Products of Cat^2Cl and Its Analogues with Methyl, *n*-Butyl, and *tert*-Butyl Substituents[a]

		phenyl (= Cat^2)		methyl		butyl		*tert*-butyl	
species[b]	ion	*m*/*z*	%	*m*/*z*	%	*m*/*z*	%	*m*/*z*	%
Cat	$[Cat]^+$	408	1	284	8	368	1	368	–
I	$[CatO]^+$	424		300		384		384	100
II	$[Cat_2OH]^+$	833	4	585	13	753	1	792[c]	65
III	$[Cat_2CO_3H]^+$	877		629		797		797	
IV	$[Cat_3CO_3]^+$	1284	100	912	100	1164	100	1164	

[a] Listed *m*/*z* values are related to ^{120}Sn, but centroid peaks in mass spectra are shifted by two (for two tin atoms, species II and III) or four (for three tin atoms, species IV) mass units. [b] See Figure 6 for structures of species I, II, III, and IV. [c] Adduct ion with acetonitrile $[Cat_2OH + acetonitrile]^+$.

mass spectra characterize the anionic parts. MS^n analyses yield fragment-rich product ion mass spectra with a predictable fragmentation. Based on the interpretation of all mass spectra, complete fragmentation patterns can be proposed and confirmed using deuterated analogues. This ESI-MS approach is routinely used in our laboratory for fast identification and reaction course screening of new synthesized organotin(IV) compounds and their hydrolysis products, because it offers distinct advantages over other spectroscopic techniques presently used for that purpose, such as X-ray diffraction and NMR spectroscopy. X-ray diffraction is the most powerful technique for the structural analysis, but the problems with obtaining monocrystals may occur. NMR spectroscopy is a standard technique for structural elucidation of organotin compounds, but it requires larger amounts of samples and high purity and can be applied only for compounds containing NMR-active nucleus. ESI-MS is a fast and relatively simple alternative technique for that purpose, but on the other hand, it cannot provide detailed information about positional isomerism or tautomerism. In our opinion, the combination of NMR, X-ray, and the novel ESI-MS approach described in this work is the most powerful tool for the unambiguous structure elucidation of complex organotin(IV) compounds. The potential of $ESI\text{-}MS^n$ is demonstrated in this work on the identification of unexpected hydrolysis products of Cat^2Cl.

ACKNOWLEDGMENT

This work was funded by research projects 203/03/1071 sponsored by the Grant Agency of the Czech Republic and MSM0021627502 sponsored by The Ministry of Education, Youth and Sports of the Czech Republic. The authors thank Libor Dostál, Petr Novák, and Zdeňka Padělková (University of Pardubice, the Czech Republic) for syntheses of studied compounds, Dr. Miroslav

Polášek (J. Heyrovský Institute of Physical Chemistry, Academy of Sciences of the Czech Republic) for fruitful discussions concerning the fragmentation mechanisms, and Prof. František Tureček (University of Washington) for critical reading of the manuscript.

SUPPORTING INFORMATION AVAILABLE

Proposed fragmentation mechanisms of Cat^2 (Figure S-1), D_6-Cat^2 (Figure S-2), D_{10}-Cat^2 (Figure S-3), D_{16}-Cat^2 (Figure S-4), Cat^3 (Figure S-5), An^8 (Figure S-6), An^9 (Figure S-7), and An^{10} (Figure S-8). This material is available free of charge via the Internet at http://pubs.acs.org.

Received for review February 9, 2006. Accepted March 27, 2006.

AC060263X